International Journal of GEOMATE, Sep., 2025 Vol.29, Issue 133, pp.147-156
ISSN: 2186-2982 (P), 2186-2990 (O), Japan, DOI: https://doi.org/10.21660/2025.133.5051
Geotechnique, Construction Materials and Environment

EXPERIMENTAL STUDY ON RIBBED BRIDGE DECK PANELS INCORPORATING HIGH-PERFORMANCE CONCRETE AND PRESTRESSING

Dang-Tung Khuc[1], Quoc-Bao Bui[2], Ba-Danh Le[1], Nho-Cang Dinh[2] and *Thi-Nguyet-Hang Nguyen[1]

[1] Faculty of Bridge and Road Engineering, Hanoi University of Civil Engineering, Vietnam
[2] Consultancy Company limited of University of Civil Engineering, Hanoi, Vietnam

*Corresponding Author, Received: 18 May 2025, Revised: 09 June 2025, Accepted: 11 June 2025

ABSTRACT: This study evaluates the structural performance of a novel precast ribbed bridge deck slab system constructed with high-performance concrete (HPC) and incorporating prestressing. Designed as a cost-effective alternative to ultra-high-performance concrete (UHPC) ribbed slabs, the proposed system employs prestressing strands placed near the neutral axis to enhance tensile capacity and overall structural integrity. A full-scale transverse rib specimen was fabricated and tested under increasing loads, supported by code-based analysis and numerical modeling. The results showed that while the slab initially exhibited flexural cracking, it ultimately failed in shear at an applied load of 100.1 kN. Prestressing was found to significantly improve crack resistance, and the connection between the HPC ribs and cast-in-place fiber-reinforced concrete shear pockets remained fully intact throughout the test. Comparisons with AASHTO design provisions confirmed the slab's flexural adequacy and identified shear as the critical failure mode. These findings highlight the critical importance of shear design in HPC waffle deck slab systems to ensure structural safety and performance.

Keywords: Ribbed slabs, HPC, Prestressing, Shear failure, Bridge design

1. INTRODUCTION

Bridge deck systems are critical to the structural integrity and serviceability of modern transportation infrastructure. Among advanced systems, precast ribbed (waffle) deck slabs constructed with ultra-high-performance concrete (UHPC) have been increasingly adopted in the United States due to their exceptional mechanical performance, durability, and compatibility with accelerated bridge construction techniques [1-3]. These systems typically comprise precast panels with orthogonal rib arrangements of which transverse ribs act as primary load-bearing T-beams and longitudinal ribs provide load-sharing capacity across adjacent units [1, 4, 5]. A number of studies have investigated UHPC ribbed slabs and demonstrated their superior performance compared to conventional slab systems [6-11].

Despite their technical advantages, the adoption of UHPC waffle deck systems in developing countries is limited by their high material cost, which is approximately 10 to 15 times that of normal-strength concrete [12]. To address this cost barrier, a research group from Vietnam has conducted research to investigate the feasibility of replacing UHPC with high-performance concrete (HPC). Bui *et al.* [12] evaluated the flexural performance of waffle slabs using C70 concrete and found that while variations in stress block assumptions exist across design codes, their impact on calculated flexural capacity is minimal. Their study further emphasized that reinforcement ratio has the most significant influence on flexural strength among parameters such as concrete strength and rib spacing.

Building upon this work, Bui *et al.* [13] further investigated key design parameters affecting HPC waffle slabs. Their results showed that using waffle configurations instead of solid slabs could reduce dead loads by 20% to 42%. However, in some cases, tensile stress limits under serviceability conditions were exceeded. To address this, the researchers proposed incorporating prestressing into the HPC ribbed slab system. Preliminary analyses indicated that, within specific ranges of girder and rib spacing, the use of prestressing strands enabled the slabs to meet serviceability requirements defined in the AASHTO 2017 specifications.

Although these previous studies have contributed significantly to the understanding of HPC waffle slabs, they were limited to analytical evaluations without experimental validation. To fill this gap, the present study conducts full-scale experimental testing on a novel HPC ribbed slab incorporating prestressing. The primary objectives are to evaluate the structural performance of the system under increasing loads and to assess its feasibility for bridge engineering applications. This paper presents a comprehensive experimental program, followed by detailed analysis of the test results, code-based calculations, and numerical modeling to provide a robust assessment of the proposed system's structural behavior.

2. RESEARCH SIGNIFICANCE

This research introduces a cost-effective alternative to UHPC waffle decks through the development of a high-performance HPC ribbed slab system. The proposed design offers innovative solutions tailored to budget-conscious infrastructure projects, promoting broader adoption of precast panel technology. Experimental results identify shear as the primary failure mode, underscoring the importance of precise shear design. Furthermore, the study highlights the benefits of prestressing in improving crack resistance and tensile performance in HPC slabs, providing valuable guidance for future designs. Overall, the research supports the creation of durable, efficient, and economical bridge decks, contributing to more sustainable and accessible infrastructure.

3. NOVEL DESIGN FOR RIBBED BRIDGE DECK PANELS USING HPC AND PRESTRESSING

It should be noted that in the design of precast slabs for bridge systems, the term slab refers to the horizontal structural element placed above girders, while "panel" typically denotes a precast subdivision of the slab system. A precast slab consists of multiple panels connected to each other through cast-in-place joints. An overview of precast UHPC ribbed (waffle) deck panels designed by the Federal Highway Administration (FHWA) is provided in previous studies [1, 4] and illustrated in Fig. 1. These ribbed deck slabs consist of waffle-shaped precast panels made from UHPC, which are connected both longitudinally and transversely along the bridge. The connections and shear pockets, also made of UHPC, are cast in place on site. In the waffle deck system, the transverse ribs (main ribs) act as T-beams, directly supporting loads such as dead and live loads, and transferring them to the main girders [1, 12]. Meanwhile, the longitudinal ribs help distribute loads to adjacent precast panels through the joint system [1].

To reduce material costs, this study proposes a novel design for ribbed bridge deck panels using high-performance concrete (HPC) with a compressive strength of 70 MPa, which is approximately twice the cost of normal-strength concrete (30–50 MPa) but significantly more economical than UHPC. However, Bui *et al.* [13] found that replacing UHPC with HPC in waffle deck panels can lead to tensile stresses at the top and bottom extreme fibers that exceed the concrete's tensile strength, thereby violating the Service Limit State requirements outlined in the AASHTO 2017 Specifications [14]. To address this issue, the proposed design incorporates prestressing near the neutral axis to introduce pre-compression across the section. The conceptual design is illustrated in Fig. 2.

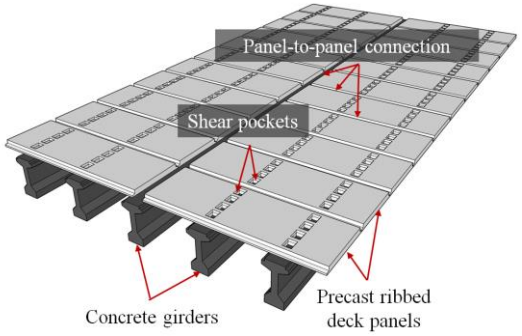

Fig. 1 Ribbed bridge deck slabs in the bridge superstructure

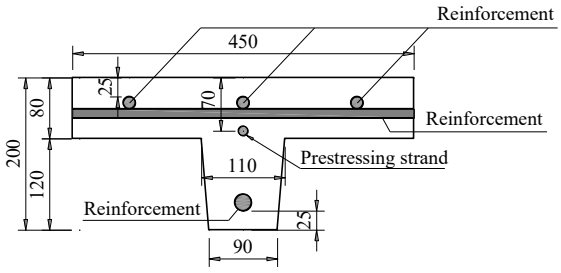

Fig. 2 Cross-section of the proposed transverse rib in novel design of a ribbed bridge deck using HPC and prestressing steel

Fig. 2 illustrates the proposed configuration of the ribbed bridge deck panel, which incorporates prestressing strands along with conventional reinforcement. This design is suitable for bridge decks with main girder spacings ranging from approximately 1.8 m to 2.8 m. The prestressing strands are positioned near the neutral axis to generate uniform pre-compressive stress across the panel, enhancing tensile performance and ensuring compliance with Service Limit State requirements. Conventional reinforcement is placed at both the top and bottom regions to effectively resist bending moments. The section details highlight the design's emphasis on achieving an economical yet structurally robust solution, particularly for use in regions where the high cost of UHPC limits its application.

To evaluate the bearing capacity of the proposed design, an experimental program was conducted. The details of this program and the corresponding test results are presented in the following sections.

4. EXPERIMENTAL PROGRAM

4.1 Specimen Configuration

Fig. 3 shows the proposed configuration of the HPC ribbed bridge deck panel (exterior panel),

measuring 6 m in length and 2.1 m in width. The bottom view (Fig. 3(b)) illustrates the arrangement of the transverse and longitudinal ribs, which form the waffle structure characteristic of the ribbed deck system. In this system, the transverse ribs, spaced at 450 mm intervals, serve as the primary load-carrying elements, directly supporting dead loads and transferring live loads to the main girders.

The design of waffle deck slabs is commonly based on the analysis of a single transverse rib cut from a precast panel. The transverse ribs act as continuous beams supported by the main girders. Fig. 4(a) shows a transverse rib extracted from the panel, while Fig. 4(b) presents details of its cross-section. As shown in Fig. 4(b), the main reinforcement for resisting hogging moments is provided by three D16 bars spaced at 150 mm, while reinforcement for sagging moments is provided by a D22 bar located at the bottom of the rib. Prestressing strands are positioned near the neutral axis to introduce uniform compressive stress throughout the section. This design aims to ensure that the panel meets structural demands while controlling cracking and enhancing durability.

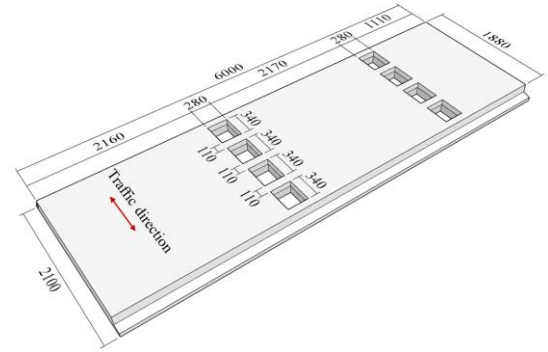

(a)

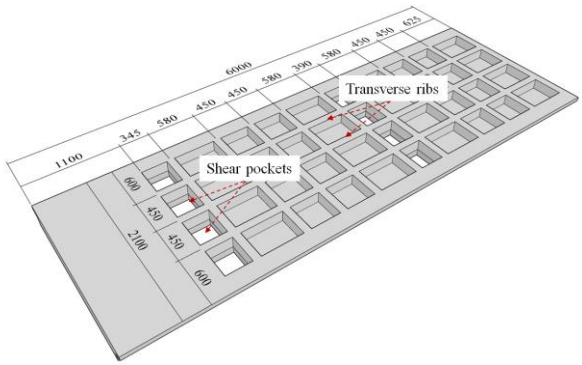

(b)

Fig. 3 Details of investigated precast exterior panel: (a) Top view; (b) Bottom view

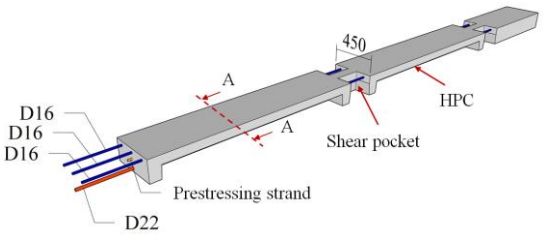

(a)

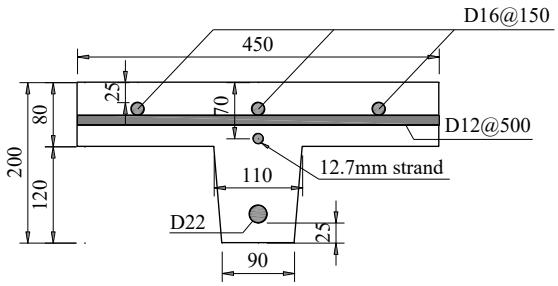

(b)

Fig. 4 Details of the test specimen: (a) 3D view of the test specimen; (b) Details of Section A-A

4.2 Specimen Preparation

A full-scale HPC transverse rib, with detailed section properties shown in Fig. 4, was fabricated for testing. Formwork was assembled, reinforcement was placed, the 12.7 mm diameter prestressing strands were stressed, and concrete with a design compressive strength of 70 MPa was cast, as shown in Fig. 5. Additionally, three concrete blocks to support the HPC rib and to simulate the working conditions of the shear pockets were cast. The design strength for the concrete blocks was 40 MPa, and their geometric details are shown in Fig. 6.

Fig. 5 Casting specimen with HPC

Once the HPC rib and concrete blocks reached sufficient strength (greater than 90% of their target values), they were transported to the testing site, and the cast-in-place shear pockets, reinforced with fibers, were filled, as shown in Fig. 7.

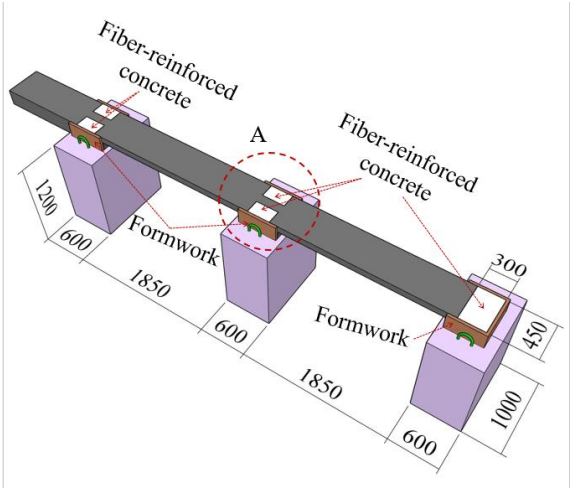

(a)

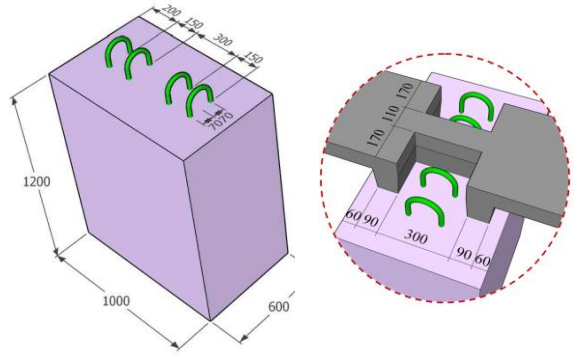

(b) (c)

Fig. 6 Details of concrete blocks: (a) Placing the HPC specimen on concrete blocks; (b) Details of concrete blocks; (c) Details of A

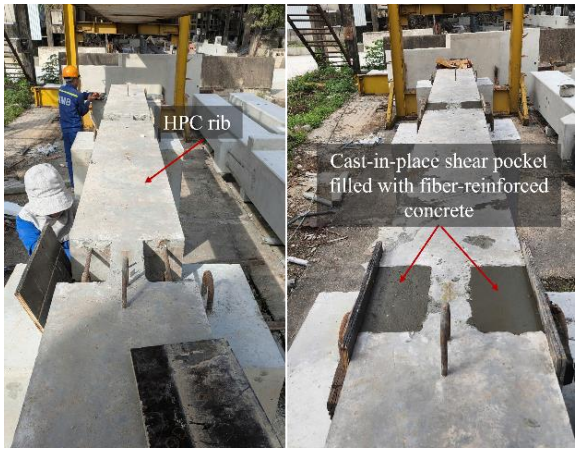

Fig. 7 Filling shear pockets with fiber-reinforced concrete

4.3 Material Properties

Table 1 presents the mix proportions used to produce 1 m³ of concrete for the HPC specimen. To evaluate the compressive strength, three cylindrical specimens (150 mm × 300 mm) were cast and tested at 28 days. The measured compressive strengths were 75.6 MPa, 76.3 MPa, and 81.4 MPa, resulting in an average strength of 77.8 MPa which was well above the design target of 70 MPa.

Table 1. Mix proportion for 1 m^3 HPC

Sand (kg)	Cement (kg)	Crushed stone (kg)	Water (kg)	Silica fume (kg)	Sika ACE 8588 (liters)
790	557	1040	130	30	6.1

For the shear pockets, a fiber-reinforced concrete mix was used, consisting of non-shrink grout, water, and high-strength steel fibers (13 mm in length, 0.2 mm in diameter, and with a tensile strength of 2750 MPa), as shown in Fig. 8. Steel fibers were added at a dosage of 2% by volume. Compressive strength tests on three samples of the fiber-reinforced concrete yielded an average strength of 50.8 MPa.

Fig. 8 Steel fibers used for shear pockets

4.4 Test Configuration and Instrumentation

The test configuration used to evaluate the structural performance of the fabricated HPC transverse rib under maximum positive moment conditions is shown in Fig. 9. The specimen was positioned atop three concrete blocks. A concentrated load, simulating a single truck axle, was applied at midspan using a hydraulic jack. The load transmitted to the specimen was monitored by a 30-ton capacity load cell.

To monitor the deformation response of the specimen, Linear Variable Differential Transformers (LVDTs) were installed at two midspan locations, with two LVDTs placed at each location, as shown in Fig. 10. Additionally, 24 strain gauges were attached to the concrete surface at the two soffits and at mid-height of the rib (100 mm from the bottom soffit) to monitor strain development throughout the loading process (Fig. 11). Data from all sensors were recorded using a data logger and will be utilized for subsequent structural analysis.

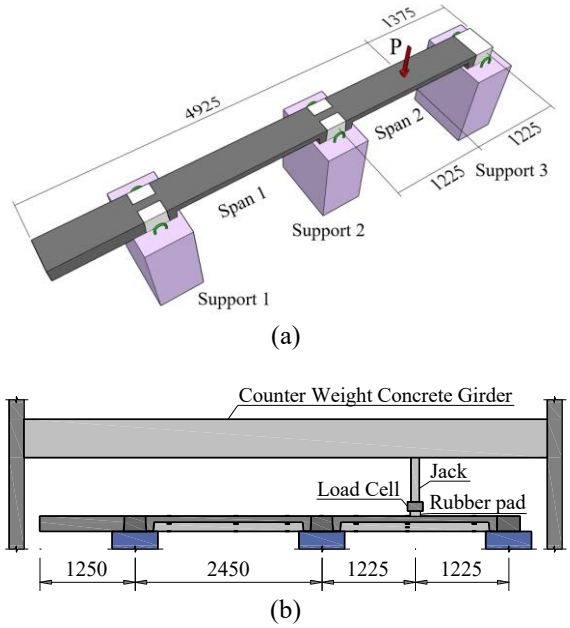

Fig. 9 Test configuration: (a) 3D view of test configuration; (b) 2D view of test setup

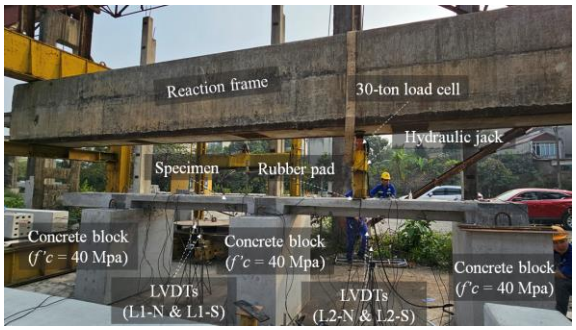

Fig. 10 Load cell and LVDT placement

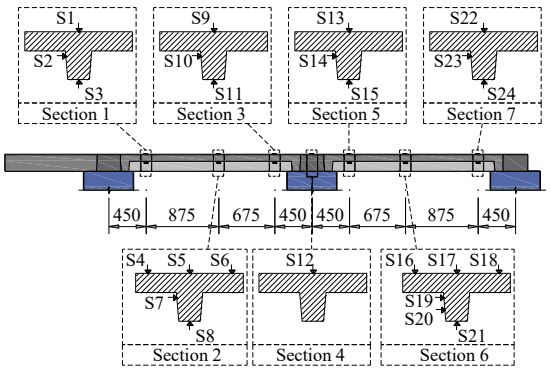

Fig. 11 Strain-gauge arrangement

5. TEST RESULTS AND DISCUSSIONS

5.1 Structural Responses

Since a hydraulic jack, rather than an actuator, was employed, the test was conducted under load control. The load increment was carefully limited to less than 5 kN. Fig. 12 presents the load-displacement curves obtained from the test, while Table 2 summarizes the key test results. It should be noted that L2-N and L2-S refer to the two LVDTs placed directly beneath the applied load location, whereas L1-N and L1-S were positioned at the midpoint of the adjacent span.

As shown in Fig. 12, initial flexural cracking was observed at an applied load of 35.8 kN, marking the first significant deviation from linear behavior. These flexural cracks appeared in the bottom region of the HPC rib, indicating the initiation of tensile stress exceedance in the concrete. As the applied load increased, additional flexural cracks formed and propagated toward the top flange. At an applied load of 90 kN, the flexural cracks extended into the top flange region, with the measured crack width reaching 0.4 mm, suggesting significant flexural behavior and increasing crack severity (Fig. 13(a)).

As the load increased to 100.1 kN, sudden shear cracks formed on the side facing the adjacent span, suggesting the imminent onset of failure. The emergence of these shear cracks indicated a shift in the failure mode from flexural to shear-dominated behavior. At this stage, the ribbed slab was considered to have failed in shear. To avoid potential damage to the LVDTs due to severe cracking, the devices were removed, marking the final recorded displacement data, although load measurements continued beyond this point. The test was concluded at an applied load of 139.9 kN, following a sudden drop in load-carrying capacity. This final failure was characterized by extensive shear cracking (Fig. 13(b)) and a significant reduction in the structure's ability to resist additional loading.

Overall, the test results demonstrate that the HPC rib initially exhibited flexural behavior; however, in the later stages, shear cracks developed, ultimately leading to a shear-dominated failure.

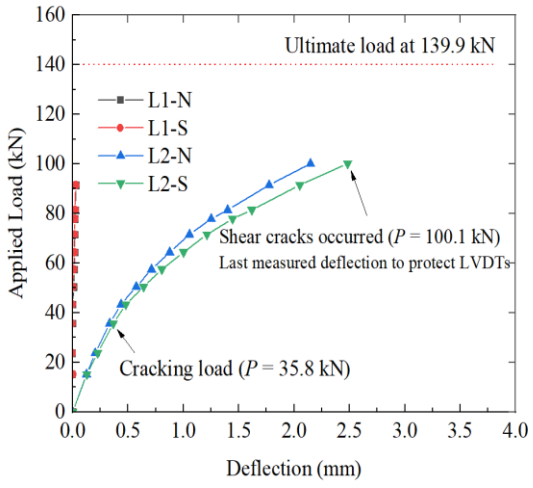

Fig. 12 Load-displacement response

Table 2. Test results

Cracking load (kN)	Failure load (kN)*	Ultimate load (kN)	Failure mode
35.8	100.1	139.9	shear

* Notable shear cracks occurred

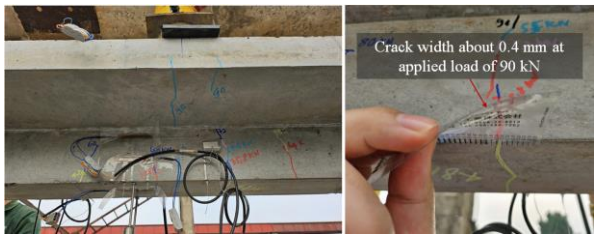

(a)

(b)

Fig. 13 Crack development and failure mode: (a) Flexural cracks progressively developed as the load increased up to 90 kN; (b) Shear failure

5.2 Concrete Strains

Strain measurements obtained from gauges attached to the concrete are presented in Figs. 14 to 18. The data show that strains at Sections 1, 2, and 3 of Span 1, the unloaded span, as depicted in Fig. 9(a), were considerably lower than those recorded at Sections 5, 6, and 7 of Span 2, where the load was directly applied. Notably, at Sections 5 and 7, tensile strains were observed at the top soffit, while compressive strains developed at the bottom soffit. This strain distribution indicates the presence of negative bending moments near Supports 2 and 3. These observations suggest limited load transfer across the second support, implying that the shear pockets functioned more like fixed supports rather than pinned supports.

The strain data can serve as a valuable resource for future research, particularly in determining the location of the neutral axis and analyzing other structural behaviors under increasing load. However, it is important to recognize that concrete strain measurements are generally more reliable before the onset of cracking. Once cracks begin to form, the strain distribution becomes non-uniform, and the measurements may no longer accurately reflect the true behavior of the concrete. Therefore, any interpretation of strain data should be conducted in conjunction with an assessment of crack development to ensure meaningful and accurate analysis.

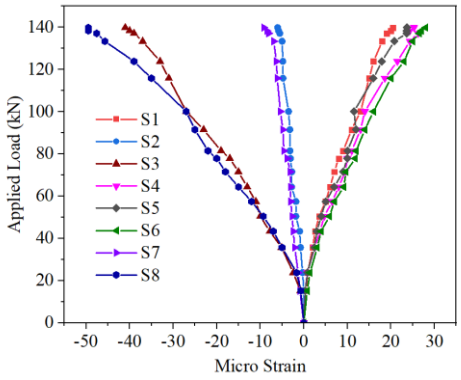

Fig. 14 Measured concrete strains - Sections 1 and 2

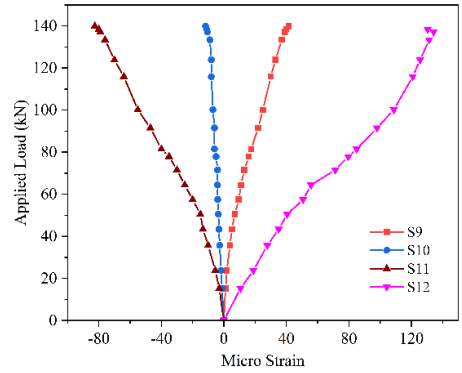

Fig. 15 Measured concrete strains - Sections 3 and 4

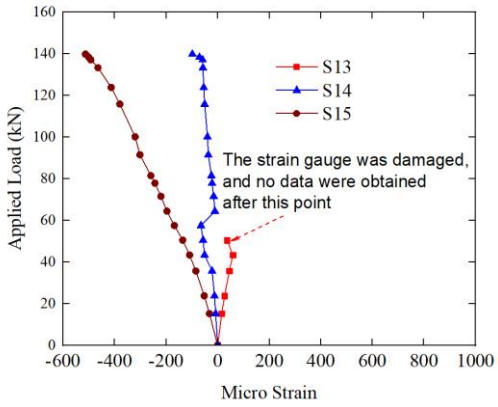

Fig. 16 Measured concrete strains – Section 5

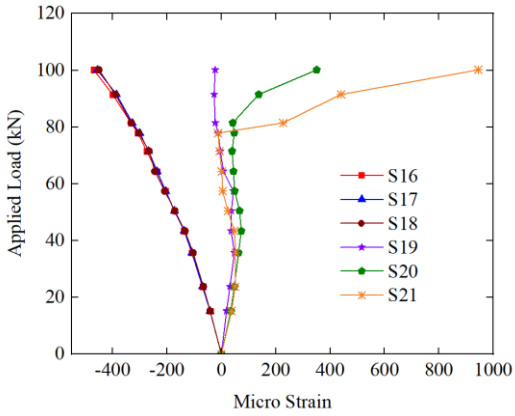

Fig. 17 Measured concrete strains – Section 6

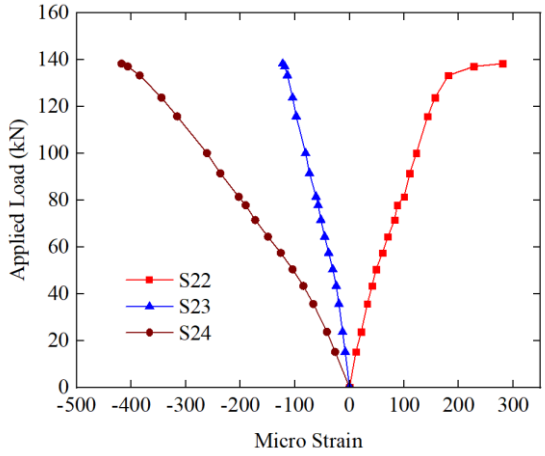

Fig. 18 Measured concrete strains - Section 7

5.3 Effectiveness of Using Prestressing

Test observations indicated that Section 7 remained uncracked under applied loads up to 133.4 kN, as evidenced by the smooth and continuous strain curves presented in Fig. 18. Consequently, the effectiveness of prestressing in the HPC ribbed slab is assessed based on the strain measurements from this section. At a load of 133.4 kN, the concrete strain at the soffit, recorded by gauge S22 in Section 7, was approximately 181 microstrain, as shown in Fig. 18.

For the tested HPC slab, which had an average concrete compressive strength of 77.8 MPa, the elastic modulus was calculated as 42.16 GPa and the tensile strength as 5.32 MPa, according to AASHTO (2017) [14]. Based on Hooke's Law, and in the absence of prestressing, concrete would be expected to crack at a tensile strain of approximately 126 microstrain. However, due to the presence of a single 12.7 mm prestressing strand embedded in the slab, the tensile stress at the bottom soffit reached up to 7.6 MPa without any visible cracking. This indicates that the prestressing effectively enhanced the slab's tensile capacity and significantly delayed the initiation of cracking, thereby confirming its beneficial role in the structural performance of HPC ribbed slabs.

5.4 Connection between HPC Rib and Shear Pockets

The integrity of the connection between the high-performance concrete (HPC) rib and the cast-in-place, fiber-reinforced shear pockets was another key focus of this investigation. Despite the shear-dominated failure observed at an applied load of 100.1 kN, and subsequent loading extended up to 139.9 kN, post-failure inspection revealed that the connection remained fully intact, with no signs of debonding or slippage (Fig. 19). This observation highlights the effectiveness of the shear pocket design and the critical role of fiber-reinforced concrete in facilitating load transfer and maintaining structural continuity.

The robust connection performance suggests that the use of high-strength steel fibers (with tensile strength of 2750 MPa) at a dosage of 7.9% by weight effectively enhanced the shear transfer mechanism at the interface. Additionally, the geometric interlock and confinement provided by the surrounding HPC ribs likely prevented crack propagation through the joint region.

Maintaining the integrity of these connections even after global failure indicates that they are not the weak link in the system and can be relied upon in practice to ensure load transfer between precast elements. This finding validates the proposed connection detail and supports its implementation in future designs, particularly for bridge applications where rapid construction and long-term durability are critical.

Fig. 19 Connection was maintained after failure

6. STRENGTH OF RIBBED SLAB USING HPC AND PRESTRESSING

6.1 Experimental Shear and Moment Capacities

The shear and moment capacities of the tested slabs were evaluated using the commercial software Midas Civil 2022. The ribbed slabs were modeled as frame elements and subjected to the loading scheme illustrated in Fig. 9. During testing, significant shear cracking was observed at an applied load of 100.1 kN. Given that shear failure is inherently brittle and abrupt, it is reasonable to consider the slab to have failed in shear at this load level, even though the test ultimately reached a maximum load of 139.9 kN. This conservative assumption is adopted to prioritize safety in both design and structural assessment.

As discussed in Section 5.2.2, the presence of negative moments at Supports 2 and 3 indicates that the beam-to-slab connections behaved more like fixed supports rather than idealized pinned connections. Therefore, in the modeling, these connections were assumed to be fixed. Fig. 20 shows the resulting shear and moment diagrams for the tested ribbed slab under the applied load of 100.1 kN, with fixed-end support conditions.

As illustrated in Fig. 20, the shear force in the slab at 100.1 kN applied load is 49.9 kN, which can be taken as the experimental shear capacity. Since

the observed failure was governed by shear rather than flexure, the slab's moment capacity must exceed the maximum observed moment demands: 27.6 kNm (positive moment) and 34.5 kNm (negative moment), as shown in Fig. 20(b). These values will be used as benchmarks for comparison with theoretical predictions based on design codes and applied loading conditions from dead and live loads in Secs 6.2 and 6.3, respectively.

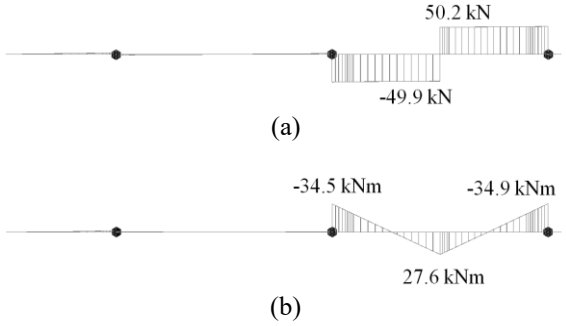

Fig. 20 Force diagram under an applied load of 100.1 kN, assuming fixed beam-to-slab connections: (a) Shear diagram; (b) Moment diagram

6.2 Shear and Moment Capacities Predicted by AASHTO 2017

To validate the experimental findings, the shear and moment capacities of the tested ribbed slabs were calculated using the AASHTO 2017 design procedures. These calculations were based on the cross-sectional details shown in Fig. 4, and the results are summarized in Table 3.

Table 3. Shear and moment capacities based on AASHTO 2017

Shear capacity (kN)	Negative moment capacity (kNm)	Positive moment capacity (kNm)
20.5	53.16	41.50

As shown in Table 3, the shear capacity predicted by AASHTO 2017 is lower than the experimentally observed value. This outcome is expected, as design codes generally incorporate conservative assumptions to ensure safety. Referring to Fig. 20 and Table 3, it is evident that under a 100.1 kN applied load, the internal shear force (approximately 50 kN) exceeds the code-based shear capacity. In contrast, both the positive and negative moment demands remain below the corresponding moment capacities predicted by the code. This discrepancy explains the shear-dominated failure mode observed during testing, thereby validating the experimental findings. It should also be noted that shear failure was commonly observed in experimental studies of UHPC ribbed slabs [6, 8].

6.3 Load Effects on Ribbed Slab under Dead Load and HL-93 Live Load

To assess the structural behavior of ribbed slabs under combined dead and live loads, the HL-93 loading model specified by the AASHTO LRFD Bridge Design Specifications (2019) was applied. The analysis was conducted considering the full bridge width, with the ribbed slab supported on four longitudinal girders spaced between 1.8 m and 2.8 m. This range aligns with the girder spacing recommendations by the Federal Highway Administration (FHWA). The overhang length was assumed to be equal to half the distance between two adjacent girders.

The applied loads on the ribbed slab system included the dead load of the slab itself, a 75 mm-thick wearing surface, and the live load specified by the AASHTO HL-93 design truck. The live load consists of a 145 kN axle load, represented by two 72.5 kN concentrated loads spaced 1.8 meters apart in the transverse direction. This configuration was positioned transversely to induce the maximum shear force at the critical cross-section under investigation. In accordance with standard design assumptions (AASHTO, FHWA), the beam-to-slab connection was modeled as a pinned support. Additionally, modeling was conducted by the authors and results demonstrate that the internal forces caused by the dead load and HL-93 live load effects are higher when using a pinned support compared to a fixed support. Therefore, for a conservative comparison, pinned supports were adopted to determine the maximum internal forces due to the dead load and live load acting on the ribbed slabs.

Figs. 21 and 22 present the resulting shear and moment envelope diagrams from Midas Civil 2022, respectively, under Strength I Limit State. Two scenarios of girder spacing (1.8 m and 2.8 m) were analyzed to analyze the ultimate internal force on individual ribs. The values shown in the figures represent the factored internal forces acting on one rib, incorporating impact effect.

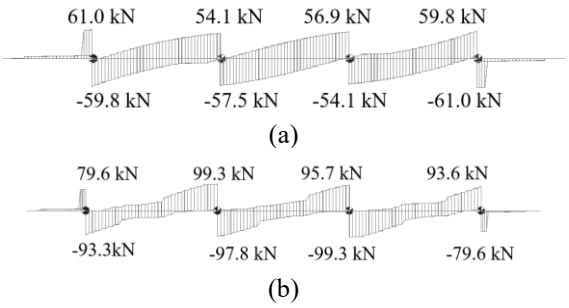

Fig. 21 Shear envelop diagram due to applied loads: (a) With girder spacing of 1.8 m; (b) With girder spacing of 2.8 m

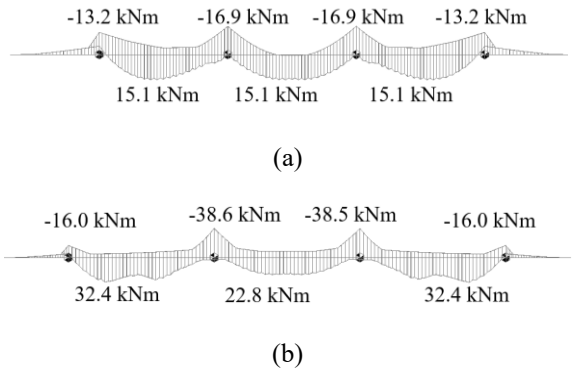

Fig. 22 Moment envelop diagram due to applied loads: (a) With girder spacing of 1.8 m; (b) With girder spacing of 2.8 m

6.3.1 Shear behavior

As shown in Fig. 21, the maximum shear force increases significantly with girder spacing. At a spacing of 1.8 m, the peak shear force reaches 61.0 kN, while at 2.8 m, it rises to 99.3 kN. These values exceed both the code-based shear capacity (20.2 kN) and the experimentally determined capacity (49.9 kN) of the ribbed slab system, as presented in Sec. 6.1. This highlights that shear is a critical design consideration for ribbed slabs constructed with high-performance concrete. Consequently, when replacing UHPC with HPC in ribbed slab designs, appropriate measures such as shear reinforcement, shear strengthening, or overall design optimization must be implemented to ensure structural safety.

6.3.2 Flexural behavior

Fig. 22 presents the moment envelope diagrams along the ribbed slab under the combined effects of dead and live loads. For a girder spacing of 1.8 m, the maximum positive and negative bending moments are 15.1 kNm and 16.9 kNm, respectively. These values increase to 32.4 kNm (positive) and 38.6 kNm (negative) for a spacing of 2.8 m. Since the ribbed slabs did not exhibit flexural failure during testing, experimental moment capacities were not determined. Therefore, moment capacities calculated using the AASHTO 2017 provisions are used for comparison. The calculated flexural capacities exceed the moment demands induced by the combined dead load and HL-93 live load, indicating that flexural failure is not a critical concern for HPC ribbed slabs. Even with increased girder spacing, minor adjustments to the reinforcement, such as increasing the bar diameter or quantity, are sufficient to ensure that the section's moment capacity surpasses the design demand.

7. CONCLUSIONS

This study investigated the structural performance of a novel precast ribbed bridge deck slab system constructed with high-performance concrete (HPC) and prestressing. The investigation involved full-scale experimental testing of a transverse rib specimen, supported by numerical modeling and theoretical analysis. Based on the results, the following conclusions are drawn:

- The experimental results demonstrated that shear was the dominant failure mechanism. Initial flexural cracking occurred at 35.8 kN, followed by progressive crack propagation up to 90 kN. A brittle shear failure occurred at 100.1 kN, highlighting the critical influence of shear in HPC ribbed slab systems.
- The interface between the HPC ribs and fiber-reinforced concrete shear pockets remained fully bonded and intact after failure, with no evidence of debonding or slippage. This confirms the effectiveness of using fiber-reinforced concrete in the connection regions.
- The use of prestressing enhanced the tensile capacity of the slab and significantly delayed crack initiation, contributing positively to serviceability. Although not experimentally assessed, the use of prestress in HPC slabs suggests potential improvements in durability.
- Strain measurements reflected the fixed-end support conditions imposed by the experimental setup, which resulted in negative moments at interior and exterior supports. However, for practical design purposes, these connections may be conservatively modeled as pinned.
- The flexural capacity of the slab was found to exceed the demands induced by dead and live loads, even at increased girder spacing, showing that flexural performance of HPC ribbed slabs is not a major concern.

In summary, the proposed HPC ribbed slab system with prestressing exhibited potential. However, particular attention must be given to the shear design to ensure safety and performance under service and ultimate loading conditions.

8. ACKNOWLEDGMENTS

This research is funded by the Ministry of Education and Training, Vietnam under grand number B2023-XDA-02.

9. REFERENCES

[1] Aaleti S., Petersen P., and Sritharan S., Design Guide for Precast UHPC Waffle Deck Panel System, including Connections – FHWA-HIF-13-032. Federal Highway Administration (USA), 2013, pp.1-127.

[2] Nguyen N.L. and Luong V.H., Mechanical and Shrinkage Behavior of Basalt Fiber Reinforced Ultra-High-Performance Concrete. International Journal of GEOMATE, Vol. 20, Issue 78, 2021,

pp.28-35.
https://doi.org/10.21660/2021.78.86151

[3] Dahish H. A. and Bakri M., Flexural Behavior of RC Composite Beams with Ultrahigh Performance Fiber Reinforced Concrete Layer Using Finite Element Modeling. International Journal of GEOMATE, Vol. 22, Issue 93, 2022, pp.75-82.
https://doi.org/10.21660/2022.93.3089

[4] Aaleti S. and Sritharan S., Design of Ultrahigh-Performance Concrete Waffle Deck for Accelerated Bridge Construction. Transportation Research Record: Journal of the Transportation Research Board, Vol. 2406, Issue 1, 2014, pp. 12-22. https://doi.org/10.3141/2406-02

[5] Honarvar E., Sritharan S., Rouse J.M., and Aaleti S., Bridge decks with precast UHPC waffle panels: A field evaluation and design optimization. Journal of Bridge Engineering, ASCE, Vol. 21, Issue 1, 2025, pp. 04015030. https://doi.org/10.1061/(ASCE)BE.1943-5592.0000775

[6] Saleem M.A., Mirmiran A., Jun X., and Mackie K., Ultra High Performance Concrete Bridge Decks Reinforced with High-Strength Steel or Fiber Reinforced Polymers. Structures Congress 2012, pp.718-734.
https://doi.org/10.1061/9780784412367.065

[7] Jinsong Z., Jingnan D., and Wang Y., Numerical and Theoretical Studies on Shear Behavior of Steel-UHPC Composite Beams with Waffle Slab. Journal of Building Engineering, Vol. 47, Issue April, 2022, pp. 103913.
https://doi.org/10.1016/j.jobe.2021.103913

[8] Saleem M.A., Mirmiran A., Jun X., and Mackie K., Experimental Characterization of Ultrahigh-Performance Concrete Bridge Deck System. Journal of Bridge Engineering, Vol. 20, Issue 9, 2014, pp. 04014101.
https://doi.org/10.1061/(ASCE)BE.1943-5592.0000697

[9] Zhu J.S., Wang Y.G., Yan J.B., and Guo X.Y., Shear Behaviour of Steel-UHPC Composite Beams in Waffle Bridge Deck. Composite Structures, Vol. 234, Issue Feb 2020, pp. 111678 https://doi.org/10.1016/j.compstruct.2019.111678.

[10] Wang K., Zhao C., Wu B., Deng K., and Cui B., Fully-Scale Test and Analysis of Fully Dry-Connected Prefabricated Steel-UHPC Composite Beam under Hogging Moments. Engineering Structures, Vol. 197, Issue Oct 2019, pp. 109380. https://doi.org/10.1016/j.engstruct.2019.109380.

[11] Baghi H., Menkulasi F., Parker J., and Barros J. A. O., Development of a High-Performance Concrete Deck for Louisiana's Movable Bridges: Numerical Study. Journal of Bridge Engineering, Vol. 22, Issue 7, 2017, pp. 04017028.
https://doi.org/10.1061/(ASCE)BE.1943-5592.0001056.

[12] Bui Q. B., Nguyen T. N. H., Khuc D. T., Nguyen T. H., Nguyen C. T., and Vu M. T., Study on the Flexural Resistance of Precast Waffle Deck Slabs Fabricated using High-Performance Concrete. Journal of Science and Technology in Civil Engineering (JSTCE) - HUCE, Vol. 18, Issue 4V, 2024, pp. 1-16.
https://doi.org/10.31814/stce.huce2024-18(4V)-01.

[13] Bui Q. B., Nguyen T. N. H., Dinh N. C., and Khuc D. T., Investigation of Design Parameters for Waffle Deck Slabs using High-Performance Concrete. Transportation and Communications Science Journal, Vol 76, Issue 02, 2025, pp. 124-138. https://doi.org/10.47869/tcsj.76.2.1.

[14] AASHTO, AASHTO LRFD bridge design specifications, American Association of State Highway and Transportation Officials USA, 2017, pp.5.1-5.260